EAST EUROPEAN JOURNAL OF PHYSICS. 4. 620-626 (2025)
DOI:10.26565/2312-4334-2025-4-65 ISSN 2312-4334

THE IMPACT OF VARIOUS LIGHTING CONDITIONS ON THE PHOTOSENSITIVE PROPERTIES OF SI<B,S> AND SI<B,Rh> STRUCTURES

Akramjon Y. Boboev[1], Shakhriyor Kh. Yulchiev[2], Ziyodjon M. Ibrokhimov[3], Nuritdin Y. Yunusaliyev[1]
[1]*Andijan State University, named after Z.M. Babur, Andijan, Uzbekistan*
[2]*Andijan State Pedagogical Institute, Andijan, Uzbekistan*
[3]*Andijan State Technical Institute, Uzbekistan*
**Corresponding Author e-mail: aboboevscp@gmail.com*
Received July 25, 2025; revised November 4, 2025; in final form November 10, 2025; accepted November 13, 2025

The paper analyses the results of experimental studies investigating the photosensitive properties of Si<B,S> and Si<B,Rh> structures under the influence of various types of radiation. It was found that the sensitivity of photodiodes fabricated based on Si<B,S> and Si<B,Rh>, increases several times (from 0.35 to 2.6 $A\cdot W^{-1}$) at decreasing temperature (from 300 K to 77 K). The threshold sensitivity of Si<B,S> based photodetectors was found to be significantly higher compared to Si<B,Rh> based photodetectors ($\Phi \approx 1.2\cdot 10^{-11}$ $lm\cdot Hz^{-1/2}$). Increasing the concentration of sulphur (S) or rhodium (Rh) in silicon increases photosensitivity, but sensitivity decreases by 3-4 times when the permissible concentration is exceeded ($N_{Rh} > 2.6\cdot 10^{15}$ cm^{-3}). It was found that photodetectors based on Si<B,S> and Si<B,Rh> retain their sensitivity parameters at high levels of radiation exposure (from protons, neutrons, electrons, and γ-quanta). In diodes based on p^+-n-p-n^+, an S-shaped I-V characteristic is observed, as well as the disappearance of the gating voltage ($U_{sp} = 0.5\div 10$ V) with increasing temperature. Relaxation of photoconductivity in diodes based on Si<B,S> and Si<B,Rh> is due to increased charge-carrier lifetimes.
Keywords: *Sulfur; Rhodium; Photoconductivity; Dopant concentration; Radiation; Monochromatic Sensitivity; Relaxation*
PACS: 85.60.Dw

INTRODUCTION

Improving the photoelectric properties of silicon through doping is crucial to the development of modern electronic devices such as photodetectors, photodiodes, and radiation sensors. Purposeful modification of the silicon structure, namely, doping it with various donor and acceptor elements, allows for control over its carrier concentration, permitted energy states, and optical sensitivity. This significantly enhances the sensitivity, reliability, and stability of devices produced on the base of silicon. In particular, doping with elements such as sulfur (S) or rhodium (Rh) leads to the formation of a p^+ layer on the surface of the silicon [1]. This particular layer serves as a reliable hole-type carrier source, enhancing efficient photoelectric control at the surface upon illumination [2]. The configuration enables the production of both p^+-i-p^+ and p^+-i-n^+ asymmetric and symmetric photodetector structures. These structures are widely used in conventional photodetectors, radiation-resistant sensors, infrared detectors, night-vision imaging systems, astronomical instruments, and high-precision devices [3]. The use of intrinsic (i-) material layers in this design shows that light doping together with quasi-intrinsic behavior enhances the well-defined, and highly efficient photoelectric effect [4].

Silicon obtains an n^+-layer through the encapsulation of phosphorus (P) as a donor material. The creation of p^+–i–n^+ structures become possible through this process because the built-in electric field enables quick and efficient photo generated carrier separation [5]. The sensitivity of the device along with its response speed improves through this fabrication. The devices designed through these processes and structures demonstrate operational stability regardless of temperature changes and radiation exposure levels [6]. These designs prove most appropriate for environments characterized by high levels of radiation found in nuclear power systems and within space exploration and defense industries.

MATERIALS AND METHODS

In this research, the response of Si<B,S> and Si<B,Rh>-based structures to different types of radiation was examined and analyzed from the perspective of their photosensitivity. Silicon (Si) was selected as the base material for forming p^+-i–n^+ semiconductor structures. Boron-doped p-type silicon wafers with a specific resistivity of approximately $\rho \approx 2\cdot 10$ Ω·cm were used as the starting material in the experiments. During the experimental procedures, either S or Rh solution was applied to one surface of the silicon wafer. This would generate p^+-regions of the p-type semiconductor with high hole carrier concentrations. Then donor sites were formed using applying phosphorus (P) solution to the other surface of wafer, forming an n^+- type layer. In this way, a three-layer structure was developed, that are shown as a p^+- type layer to the top of the semiconductor layer, a i-layer in the middle, and n^+-type layer to the bottom. The silicon wafers were glued together with adequate pressure to provide good electrical and physical properties between the layers. This method ensured that the dopants could be uniformly distributed in the Si crystal lattice, and were well integrated.

Cite as: A.Y. Boboev, Sh.Kh. Yulchiev, Z.M. Ibrokhimov, N.Y. Yunusaliyev, East Eur. J. Phys. 4, 620 (2025), https://doi.org/10.26565/2312-4334-2025-4-65

After the fabrication of the structures, we thermally treated them at temperatures between 1250 to 1300 °C, in diffusion atmospheres of either air or inert gases (nitrogen or argon). Thus, using the oven method to fabricate structures, the p^+ and n^+ dopants would diffuse into the silicon crystal, allowing the material to develop suitable p^+–i–n^+ structures with respect to depth.

To investigate radiation-induced modifications, irradiation experiments were carried out at the Institute of Nuclear Physics of the Academy of Sciences of the Republic of Uzbekistan (INP AS RUz). Proton irradiation was performed using the U-150-II isochronous cyclotron, which accelerates protons up to 18 MeV. Neutron irradiation was conducted using the NG-150 neutron generator, producing a quasi-monochromatic neutron flux with an energy of about 14 MeV. Electron irradiation was performed using the LINAC-1000 linear accelerator, generating electron beams with energies up to 10 MeV. All irradiation parameters – including fluence, energy, and exposure time – were precisely controlled to ensure the stability and reproducibility of the experimental conditions.

The compensation ratio $K = \bar{P}/N_S$ was evaluated using the effective carrier concentration $\bar{P}$ and the concentration of sulfur impurity N_S. The value of $\bar{P}$ was determined from the measured electrical resistivity using the expression

$$\bar{P} = \frac{1}{q \cdot \mu_p \cdot \rho} \cdot 100\%] \qquad (1)$$

where q is the elementary charge and μ_p is the hole mobility at room temperature. The sulfur concentration N_S was estimated from the diffusion profile parameters and solubility data reported for compensated crystals based on Si<B,S> in the study [1]. The sulfur concentration N_S was estimated from the diffusion profile parameters and solubility data reported for Si<B,S>-based compensated crystals in study [1].

RESULTS AND DISCUSSION

Photovoltaic characteristics

In our experimental investigations, spectral characteristics of p^+–i–p^+ and p^+–i–n^+ devices were studied by their comparison with spectral characteristics of the reference industry photodiode – FD-28KP. Thanks to experiments, it was feasible to estimate with high precision the spectral sensitivity and operating parameters for the described structures. Figures 1a and 1b depict the measured spectral sensitivity curves of the devices, and Table 1 lists the corresponding device parameters. The photodetector sensitivity was dramatically enhanced, particularly when the operating temperature was lowered to 77 K. Cooling of the operating temperature from 300 K to 77 K enhanced the spectral sensitivity of the Si<B,S> structure from $S_\lambda \approx 0.35$ A·W^{-1} to about 2.6 A·W^{-1} at a wavelength $\lambda = 0.625$ µm. In the same temperature range, the sensitivity of the Si<B,Rh> structure grew from $S_\lambda \approx 0.28$ A·W^{-1} up to about 0.74 A·W^{-1}. These facts prove that the sensitivity of these structures is enhanced several times when operating at cold (cryogenic) temperatures and thus they can be used as low-light sensors in cryogenic detector systems [7].

The minimum light sensitivities (Φ) of the photodetectors were also measured in the experiments. When a load resistance of $R_H = 50$ kΩ was employed, the corresponding Φ values of the Si<B,S> and Si<B,Rh> structures were $\Phi \approx 1.2 \cdot 10^{-11}$ lm·Hz$^{-1/2}$ and $\Phi \approx 4.0 \cdot 10^{-10}$ lm·Hz$^{-1/2}$, respectively. These extremely low Φ values evidently confirm that structures enable the detection of extremely weak light signals with high precision.

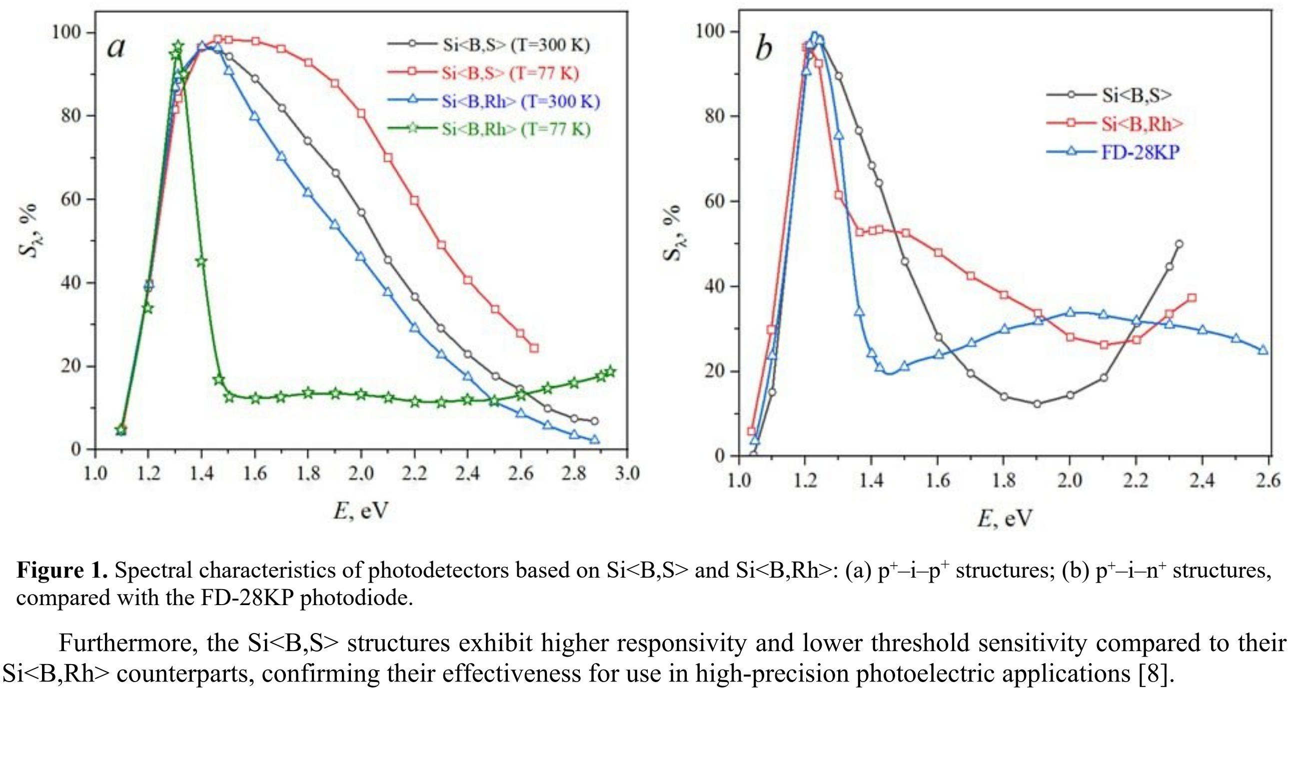

Figure 1. Spectral characteristics of photodetectors based on Si<B,S> and Si<B,Rh>: (a) p^+–i–p^+ structures; (b) p^+–i–n^+ structures, compared with the FD-28KP photodiode.

Furthermore, the Si<B,S> structures exhibit higher responsivity and lower threshold sensitivity compared to their Si<B,Rh> counterparts, confirming their effectiveness for use in high-precision photoelectric applications [8].

Table 1. Parameters of photosensitive structures based on Si<B,S> and Si<B,Rh>

no.	Parameter	Si<B,S>	Si<B,Rh>
1	Noise voltage (U_N), μV	2÷10	2÷10
2	Monochromatic sensitivity (S_λ) λ=0.85 μm, A/W	0.50÷0.75	0.50÷0.75
3	Integral current sensitivity (S_I), mA/lm	40÷50	40÷50
4	Photoresponse time constant (τ), s	$(2÷50)\cdot10^{-4}$	$(2÷50)\cdot10^{-4}$

Effect of Dopant Concentration

The conducted studies have shown that when p-type silicon is treated with sulfur (S) or rhodium (Rh), an increase in dopant concentration leads to a corresponding rise in photosensitivity. The silicon crystal lattice was able to effectively retain charge carriers under illumination, while the dopant elements helped reduce recombination effects [9]. However, when the dopant is added in excess beyond a certain threshold, an overcompensated state occurs, resulting in donor–acceptor compensation. This significantly reduces the number of free carriers [10]. Consequently, the sensitivity of the photodetectors typically drops by a factor of 3 to 4. Furthermore, this situation can lead to the formation of potential barriers within the structure, which are associated with structural defects and contribute to a reduction in photocurrent. For Si-based structures with varying Rh concentrations, the dark current (I_d**)**, measured in the absence of illumination, and the photocurrent (I_{ph}**)**, measured under illumination, are presented in Table 2. This table also illustrates the influence of Rh concentration on the photoelectric response of the structures. The data in the table show that once the Rh concentration exceeds the optimal level, the steady-state photocurrent decreases, and the I_{ph}/I_d ratio changes. When the Rh concentration is approximately $N_{Rh} \approx 2.6\cdot10^{15}$ cm^{-3}, the I_{ph}/I_d ratio reaches a value of 10^7 at a temperature of 77 K, indicating very high sensitivity. However, when Rh concentration surpasses the threshold, no further improvement in sensitivity is observed, as excessive dopant levels ultimately lead to the degradation of the functional system [12].

Table 2. Photocurrents as a function of Rh concentration

N_{Rh}, cm^{-3}	300 K			77 K		
	I_d, A	I_{ph}, A	I_{ph}/I_d	I_d, A	I_{ph}, A	I_{ph}/I_d
$7\cdot10^{14}$	$1.1\cdot10^{-4}$	$1.0\cdot10^{-3}$	9.1	$2.3\cdot10^{-6}$	$8\cdot10^{-5}$	35
$1.5\cdot10^{15}$	$4\cdot10^{-6}$	$3.8\cdot10^{-5}$	9.5			$1.6\cdot10^{6}$
$2.6\cdot10^{15}$	$1.6\cdot10^{-6}$	$1.8\cdot10^{-5}$	11	$1\cdot10^{-10}$	$1.8\cdot10^{-3}$	$1.8\cdot10^{7}$

Effect of irradiation

The effect of radiation on the sensitivity parameters (S_λ and S_I) of structures formed on the basis of Si<B,Rh> and Si<B,S> is presented in Tables 3 and 4. These tables analyze the changes in current sensitivity of the structures under the influence of various types of radiation, such as protons, neutrons, electrons, and γ-quanta. According to the experimental results, in most cases, structures based on Si<B,Rh> demonstrated a greater increase in sensitivity compared to those based on Si<B,S>. Experimental results show that Si<B,Rh> and Si<B,S>-based photodetectors retain high levels of sensitivity under γ-irradiation fluences ranging from 10^{14} cm^{-2} to approximately 10^{18} cm^{-2} (Table 3). The retention of sensitivity at such high fluence levels indicates the robustness and stability of the defect-mixture complexes formed in the crystal lattice.

Table 3. Changes in current sensitivity under the influence of radiation type and currents

no.	Type of radiation	Integral flow (cм$^{-2}$)	ΔS_I (%) Si<B,S>
1	Protons (E=18 MeV)	$5\cdot10^{12}/1\cdot10^{13}/5\cdot10^{13}$	20/50/92
2	Neutrons (E≥0.1 MeV)	$3\cdot10^{13}/5\cdot10^{13}/8\cdot10^{13}$	12/42/55
3	Electrons (E=6 MeV)	$10^{14}/10^{15}/10^{16}$	7/44/87
4	γ-quanta (^{60}Co)	$1.1\cdot10^{18}/2.5\cdot10^{18}/3.5\cdot10^{18}$	7/38/70

Table 4 presents how the key parameters — S_λ, S_I, and τ — of components based on Si<B,S> and Si<B,Rh> change before and after irradiation. Although the sensitivity of both structures decreased slightly after radiation exposure, their values remained above the industry-accepted thresholds.

Table 4. Parameters of Si<B,S> and Si<B,Rh> based structures before and after irradiation with fast neutrons

Parameter	Si<B,S> before	Si<B,S> after a fast neutron fluence of ~10^{14} cm^{-2}	Si<B,Rh> before	Si<B,Rh> after a fast neutron fluence of ~10^{14} cm^{-2}
Monochromatic sensitivity (S_λ), A/W	0.70	0.40	0.78	0.26
Integral current sensitivity (S_I), mA/lm	49.4	21	55	13.29
Photoresponse time constant (τ), s	$1\cdot10^{-4}$	$8\cdot10^{-5}$	$1\cdot10^{-4}$	$6\cdot10^{-5}$

Sensors based on Si<B,S> and Si<B,Rh> continued to operate reliably and stably even after being subjected to irradiation. These structures demonstrate notable utility for long-term wireless applications in high-radiation environments, providing a solid scientific basis for their future implementation [13].

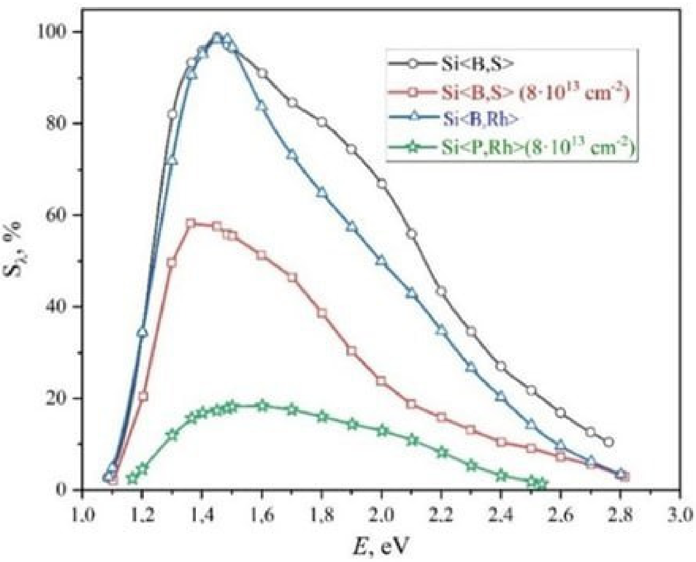

Figure 2. Spectral characteristics of Si<B,S> and Si<B,Rh> structures without irradiation and after irradiation with fast neutrons with a fluence of $8\cdot10^{13}$ cm^{-2}

The spectral characteristics shown in Figure 2 present an analysis of the photodetectors both before and after neutron irradiation. It was observed that silicon-based photodetectors containing boron and sulfur (n-Si<B,S>) demonstrated greater resistance to radiation-induced changes in spectral responsivity compared to conventional silicon counterparts. Silicon photodiodes fabricated from specially modified materials showed a neutron radiation resistance that is three to four times higher than that of standard industrial-grade photodiodes. This conclusion is further supported by the data in Table 5, which illustrates how exposure to fast neutrons (E ≥ 0.1 MeV) affects the integral current responsivity of different photodetector types. The table provides a comparative analysis of the relative change in integral responsivity - expressed as $[S_I = \frac{S_I^0 - S_I^{rad}}{S_I^0} \cdot 100\%]$ - for photodetectors based on n-Si<B,S> and the industrial reference model FD-10K. According to the results, photodetectors built on n–Si<B,S> substrates maintained stable integral responsivity over the entire irradiation range, with relative variations within 10–31%. In contrast, the FD-10K industrial photodiode exhibited a significantly larger decrease in responsivity (80–88%), indicating that its performance degrades much more strongly under neutron irradiation.Thus, the results showed that the n–Si<B,S>-based photodetectors maintain their functional stability significantly better under neutron irradiation than the FD-10K device, which indicates that they are suitable for long-term operation in environments with high radiation levels [14].

Table 5. Relative change in integral susceptibility under the influence of fast neutrons

Fluence (cm^{-2})	Si<B,S> (%)	FD-10K (%)
$2\cdot10^{13}$	10	80
$4\cdot10^{13}$	17	83
$6\cdot10^{13}$	26	86
10^{14}	31	88

A specific group of diodes fabricated using p^+–n–p–n^+ type semiconductor structures was observed to exhibit an S-shaped current - voltage (I-V) characteristic. During the experiments, it was found that these diodes undergo a sudden switching behavior, resulting in what is known as a snapback voltage (U_{sp}). When the applied voltage approached a certain critical threshold, the diode's operating state changed abruptly. It was also noted that as the temperature increased, the S-shaped portion of the I–V curve gradually disappeared, making the curve smoother overall. This behavior makes such diodes particularly well-suited for temperature-sensitive devices like photorelays and thermal sensors. The measurements showed that snapback typically occurs within a voltage range of approximately $U_{sp} \approx 0.5$ to 10 V, with the corresponding current values ranging between $I_{sp} \approx 0.2$ and 1 mA [15]. At elevated temperatures, the snapback region faded, confirming the diode's suitability for thermal-responsive switching applications [16,17]. Further investigation revealed that the magnitude of the snapback voltage is directly influenced by two internal parameters of the diode: the base resistivity (ρ) and the level of compensation (K) [18]. This relationship was explored by analyzing the $U_{sp}^{max}/U_{sp}^{min}$ ratios presented in Table 6, which reflect how changes in compensation and base resistivity affect snapback behavior. The experimental results clearly demonstrated that increasing the compensation level leads to a wider snapback voltage range. This opens up the possibility of fine-tuning diode parameters and gaining precise control over the device's switching domain. By selecting an optimal compensation level in p^+–n–p–n^+ structures, it is possible to adjust the snapback voltage to meet specific technological requirements, enabling flexible and efficient use across a wide range of real-world electronic applications [19].

Table 6. Ratio $U_{sp}^{max}/U_{sp}^{min}$ depending on ρ and compensation level

ρ, Ω·cm	$U_{sp}^{max}/U_{sp}^{min}$	$K = \overline{P}/N_S$
1	-	0.51
3	1.5	0.78
10	3.5	0.91
20	5	0.95

γ-irradiation effect and relaxation

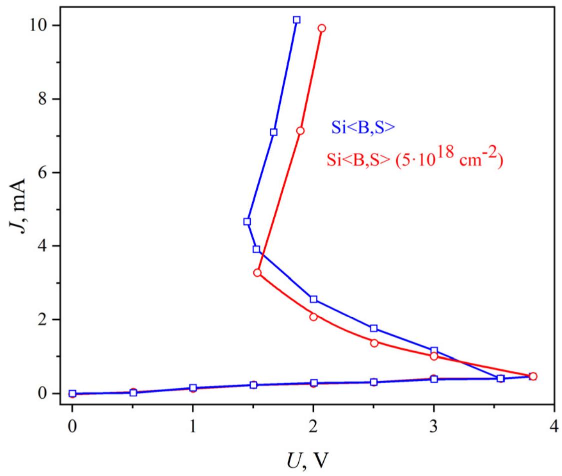

Figure 3. Current-voltage characteristics of S-diodes prepared based on Si<B,S> before and after irradiation (***γ***-irradiation)

Silicon-based S-diodes show excellent radiation resistance due to their stable performance. The (U_{sp}) and (I_{sp}) measurements of the diodes remained stable when γ-radiation from ^{60}Co had been applied according to experimental findings (Figure 3). Data findings about the material's excellent resistance to radiation confirms the evidence strongly. The research investigated photoconductivity relaxation mechanisms in either Si<B,S> or Si<B,Rh> based diodes separately. The experimental results matched previously recorded data, which indicated that the relaxation of photoconductivity depends directly on increased carrier lifetime [20].

It is known that the relaxation of photoconductivity in silicon-based materials is directly related to the lifetime of unbalanced charge carriers. After illumination is removed, the excess carriers recombine through defect trap centers located within the forbidden band gap. The recombination-generation dynamics in such systems is described by Shockley-Read-Hall (SRH) statistics, where the presence of deep-level traps, shifting the Fermi level to a position away from the recombination centers, can significantly extend the carrier lifetime by reducing the effective recombination rate. The introduction of sulfur or rhodium into the compensated Si<B,S> and Si<B,Rh> structures created local deep energy states that stabilized the unbalanced carriers, thereby increasing the relaxation time of photoconductivity and the photosensitivity. Thus, the observed long-term relaxation behavior was consistent with the SRH model and confirmed that the increase in photoconductivity is directly related to the increase in the carrier lifetime. An extended carrier lifetime improves photo detector stability through photosensitive materials when operated over extended time span [21].

The research findings demonstrate that S-diodes containing Si<B,S> and Si<B,Rh> show promising performance in high-dose radiation environments due to their reliable operation and stable photosensitivity characteristics [22].

CONCLUSIONS

Based on the analysis of experimental investigations into the effects of various types of radiation on the photosensitivity properties of Si<B,S> and Si<B,Rh> structures, the following conclusions can be drawn:

Photodiodes using Si<B,S> and Si<B,Rh> become much more sensitive – increasing several times (from 0.35 to 2.6 $A \cdot W^{-1}$) – when cooled down (from 300 K to 77 K). This makes them usable as very cold sensors and detectors for recording dim radiation.

The threshold sensitivity for Si<B,S> photodetectors is much better ($\Phi \approx 1.2 \cdot 10^{-11}$ $lm \cdot Hz^{-1/2}$) than Si<B,Rh> ones. This means they can spot really weak light signals with great precision.

More sulfur (S) or rhodium (Rh) in the silicon boosts photoelectric sensitivity. But, if you add too much ($N_{Rh} > 2.6 \cdot 10^{15}$ cm^{-3}), the sensitivity drops by 3–4 times.

Si<B,S> and Si<B,Rh> photodetectors retain their sensitivity even under high-radiation environments (protons, neutrons, electrons, and γ-rays).

In p^+–n–p–n^+ diodes, we saw an S-shaped I-V behavior and the breakdown voltage (U_{sp} = 0.5÷10 V) disappeared as the temperature went up. Because of this, these diodes can be used as very sensitive photorelays and temperature sensors.

The photoconductivity relaxation in Si<B,S> and Si<B,Rh> diodes is due to the charge-carrier lifetime increasing. This helps photodetectors remain stable for a long time, enabling reliable, effective use in environments with high radiation levels.

Conflict of Interests

The authors declare that they have no conflicts of interest.

Funding

The present research was funded by the FZ-292154210 project, granted by the Ministry of Innovative Development of the Republic of Uzbekistan.

ORCID

A.Y. Boboev, https://orcid.org/0000-0002-3963-708X; **Sh.Kh. Yulchiev,** https://orcid.org/0009-0007-2576-4276
N.Y. Yunusaliyev, https://orcid.org/0000-0003-3766-5420; **Z.M. Ibrokhimov**, https://orcid.org/0009-0003-6931-661X

REFERENCES

[1] A.Y. Boboev, Kh.A. Makhmudov, Z.M. Ibrokhimov, A.K. Rafikov, N.Y. Yunusaliyev, and S.Kh. Ibrokhimov, "Long-term relaxation processes of electrical conductivity in compensated Si<B,S> and Si<B,Rh> monocrystals," East European Journal of Physics, (2), 436–440 (2025). https://doi.org/10.26565/2312-4334-2025-2-54
[2] H. Zhang, and N.-G. Park, "Progress and issues in p-i-n type perovskite solar cells," DeCarbon, **3**, 100025 (2024). https://doi.org/10.1016/j.decarb.2023.100025
[3] K.S. Daliev, Sh.B. Utamuradova, J.J. Khamdamov, M.B. Bekmuratov, O.N. Yusupov, Sh.B. Norkulov, and Kh.J. Matchonov, "Defect Formation in MIS Structures Based on Silicon with an Impurity of Ytterbium," East Eur. J. Phys. (4), 301-304 (2024). https://doi.org/10.26565/2312-4334-2024-4-33
[4] T. Taima, M. Chikamatsu, Y. Yoshida, K. Saito, and K. Yase, "Effects of intrinsic layer thickness on solar cell parameters of organic p-i-n heterojunction photovoltaic cells," Appl. Phys. Lett., **85**(26), 6412–6414 (2004). https://doi.org/10.1063/1.1841479
[5] F.P. Ziemba, G. Pelt, G. Ryan, L. Wang, and R. Alexander, "Properties of an n+ i p+ Semiconductor Detector," IRE Trans. Nucl. Sci., 9(3), 155–159 (1962). https://doi.org/10.1109/tns2.1962.4315987
[6] S.Z. Zainabidinov, A.Y. Boboev, N.Y. Yunusaliyev, and J.N. Usmonov, "An optimized ultrasonic spray pyrolysis device for the production of metal oxide films and their morphology," East Eur. J. Phys. (3), 293 (2024). https://doi.org/10.26565/2312-4334-2024-3-30
[7] M.S. Kukurudziak, "Analysis of the Spectral Characteristics of the Responsivity of Diffusion p-i-n; Photodiode Based on High Resistivity p-Si," Microsystems, Electronics and Acoustics, **28**(1), 47-51 (2023). https://doi.org/10.20535/2523-4455.mea.275010
[8] A.S. Saidov, Sh.N. Usmonov, M.U. Kalanov, and Kh.M. Madaminov, "Effect of gamma irradiation on photoconductivity and photosensitivity of $Si_{1-x}Sn_x$ solid solutions," Heliotechnical Mater. Sci. **47**, 48–51 (2011). https://doi.org/10.3103/S0003701X11010142
[9] M. Karimov, and A. K. Karakhodzhaev, "Investigation of Si<B,S> and Si<B,Rh> compensated photoresistors," Russ. Phys. J. **43**(6), 509–511 (2000). https://doi.org/10.1007/bf02508633
[10] M. Koopmans, M.A.T. Leiviskä, J. Liu, J. Dong, L. Qiu, J. C. Hummelen, G. Portale, *et al.*, "Electrical Conductivity of Doped Organic Semiconductors Limited by Carrier–Carrier Interactions," ACS Appl. Mater. Interfaces, **12**(50), 56222–56230 (2020). https://doi.org/10.1021/acsami.0c15490
[11] H.A. Hadi, R.A. Ismail, and A.R. Abdulwahhab, "Effect of Gamma Irradiation on the Optoelectronics Properties of Porous Si/c-Si Heterojunction photodetector," Silicon, **16**(3), 1097–1106 (2023). https://doi.org/10.1007/s12633-023-02731-w
[12] A.Y. Boboev, B.M. Ergashev, N.Y. Yunusaliyev, J.S. Madaminjonov, "Electrophysical nature of defects in silicon caused by implanted platinum atoms," East Eur. J. Phys. (2), 431 (2025), https://doi.org/10.26565/2312-4334-2025-2-53
[13] Y. Wei, Ch. Lan, et al., "Recent Advances in Photodetectors Based on Two-Dimensional Material/Si Heterojunctions," Appl. Sci. **13**, 11037 (2023). https://doi.org/10.3390/app131911037V.
[14] N.K. Tailor, C.A. Aranda, *et al.*, "Negative Photoconductivity: Bizarre Physics in Semiconductors," ACS Mater. Lett. **4**(11), 2298–2320 (2022). https://doi.org/10.1021/acsmaterialslett.2c00675
[15] A.O. Goushcha, B. Tabber, *et al.*, "Silicon photoresistive sensors with improved performance," J. Appl. Phys. **123**, 044505 (2018). https://doi.org/10.1063/1.5006819
[16] G.-F. Dalla and J. Ye, "Silicon Radiation Detector Technologies: From Planar to 3D," Chips, **2**, 83–101 (2023). https://doi.org/10.3390/chips2020006
[17] W. Jiang, T. Li, L. Yin, J. Chen, D. Niu, G. Li, Y. Shi, *et al.*, "Thermal switch with tunable thermal conductivity via external stimuli and thermal diodes," Appl. Therm. Eng. **275**, 126848 (2025). https://doi.org/10.1016/j.applthermaleng.2025.126848
[18] V. Terracciano, A. Borghese, M. Boccarossa, V. d'Alessandro, and A. Irace, "A Geometry-Scalable Physically-Based SPICE Compact Model for SiC MPS Diodes Including the Snapback Mechanism," Solid State Phenom. **360**, 67–74 (2024). https://doi.org/10.4028/p-b9imzl
[19] F. Chen, D.S. Chao, M.-J. Chen, P. Yen, J.-T. Yeh, C.-M. Lee, W.-H. Wang, *et al.*, "S-shaped negative differential resistance modeling in electro-thermal simulation of phase-change memory programming," in: *Proceedings of the 2007 Non-Volatile Memory Technology Symposium (NVMT)*, 2007, pp. 67–70. https://doi.org/10.1109/NVMT.2007.4389949
[20] T. Asada, Y. Ichikawa, and M. Kato, "Carrier lifetime measurements in semiconductors through the microwave photoconductivity decay method," Journal of Visualized Experiments (JoVE), **146**, 31058909 (2019). https://doi.org/10.3791/59007
[21] C.R. Doerr, "Silicon photonic integration in telecommunications," Front. Phys. **3**(37), (2015). https://doi.org/10.3389/fphy.2015.00037
[22] M.S. Yunusov, M. Karimov, and B.L. Oksengendler, "On the mechanisms of long-term relaxation of the conductivity in compensated Si<B,S> and Si<B,Rh> as a result of irradiation," Semiconductors, **32**(3), 238–240 (1998). https://doi.org/10.1134/1.1187387

ВПЛИВ РІЗНИХ УМОВ ОСВІТЛЕННЯ НА ФОТОЧУТЛИВІ ВЛАСТИВОСТІ СТРУКТУР Si<B,S> ТА Si<B,Rh>

Акрамджон Й. Бобоєв[1], Шахріор Х. Юльчієв[2], Зіоджон М. Іброхімов[3], Нурітдін Й. Юнусалієв[1]
[1]Андижанський державний університет імені З.М. Бабура, Андижан, Узбекистан
[2]Андижанський державний педагогічний інститут, Андижан, Узбекистан
[3]Андижанський державний технічний інститут, Узбекистан

У статті проаналізовано результати експериментальних досліджень фоточутливих властивостей структур Si<B,S> та Si<B,Rh> під впливом різних видів випромінювання. Було виявлено, що чутливість фотодіодів, виготовлених на основі Si<B,S> та Si<B,Rh>, зростає в кілька разів (від 0,35 до 2,6 $А·Вт^{-1}$) при зниженні температури (від 300 К до 77 К). Порогова чутливість фотодетекторів на основі Si<B,S> виявилася значно вищою порівняно з фотодетекторами на основі Si<B,Rh> ($Ф \approx 1{,}2·10^{11}$ $лм·Гц^{-1/2}$). Збільшення концентрації сірки (S) або родію (Rh) у кремнії підвищує фоточутливість, але чутливість зменшується в 3-4 рази при перевищенні допустимої концентрації ($NRh > 2{,}6·10^{15}$ $см^{-3}$). Було виявлено, що фотодетектори на основі Si<B,S> та Si<B,Rh> зберігають свої параметри чутливості при високих рівнях радіаційного опромінення (від протонів, нейтронів, електронів та γ-квантів). У діодах на основі p^+-n-p-n^+ спостерігається S-подібна вольт-амперна характеристика, а також зникнення напруги затвора (Usp = 0,5÷10 В) зі збільшенням температури. Релаксація фотопровідності в діодах на основі Si<B,S> та Si<B,Rh> зумовлена збільшенням часу життя носіїв заряду.

Ключові слова: *сірка; родій; фотопровідність; концентрація легуючої домішки; випромінювання; монохроматична чутливість; релаксація*